

## On the Use of Inverse Analysis for the Estimation of Soil Hydraulic and Retention Parameters from Monitoring Data of a River Embankment

Ilaria Bertolini<sup>1</sup>, Carmine Gerardo Gragnano<sup>1</sup> & Guido Gottardi<sup>1</sup>

<sup>1</sup>DICAM Department, University of Bologna, viale del Risorgimento 2, Bologna, Italy  
E-mail: [ilaria.bertolini3@unibo.it](mailto:ilaria.bertolini3@unibo.it)

**Abstract:** Seepage in the vadose zone greatly depends on the hydraulic properties of the soil. Their experimental determination often requires specific equipment and time-consuming procedures; furthermore, in many applications, such as river embankments, the spatial variability of these properties turns out to be particularly significant. Although the use of a monitoring system is often an essential aspect of engineering projects, quantitative tools for the calibration of predictive models based on site measurements are not fully explored. Recently, indirect estimate of parameters through inverse analysis has proven to be a valid alternative to direct methods (i.e. site and laboratory investigations), especially in large-scale studies, in which an extensive set of input data needs to be defined. The present study proposes an in-depth investigation of limitations and potentials of inverse modelling procedures for the estimation of soil hydraulic parameters. The case study is a multi-layered river embankment section along the river Secchia, a right-hand tributary of the river Po (Northern Italy), subjected to transient seepage phenomena in saturated and unsaturated conditions due to river level fluctuations and soil-atmosphere interaction. Site monitoring of water content and pore water pressure within the riverbank body ensures a wide set of observation data to be used for the calibration of a FE flow model. Numerical simulations using different retention models combined with the local optimization method based on the Levenberg-Marquardt algorithm have been considered to perform the inverse analysis. Finally, a comparison among indirect simulation performances is presented through qualitative and quantitative methodologies.

**Keywords:** Indirect simulations; Inverse analysis, Parameters calibration, Monitoring data, River embankment.

### 1 Introduction

River flooding is a worldwide natural hazard with huge socio-economic impacts that are expected to rise due to the urbanization of flood-prone areas by an increasing world population, to the increment in property values in parallel with the global economic growth and to the effects of climate change. To meet the need of a better management of the hydrogeological risk, economic investments, time and expertise have been employed by public authorities and scientific community to deal with slope stability of unsaturated riverbanks subjected to transient boundary conditions. This problem is governed by soil strength parameters, which in turn depend on suction, water content and degree of saturation. For this reason, it is required a good and reliable estimation of such variables as a function of space and time, i.e. their distribution within the relative investigated domains (Gottardi et al. 2016; Gragnano et al. 2019). Such information are then used to set analytical and numerical models representing the phenomena under investigation and often to perform the calibration and subsequent validation phases. Despite the most diffused optimization technique still remains the qualitative “trial and error procedure”, which is time-consuming and modeller’s affected, a quantitative parameters estimation, such as the inverse analysis, has recently become a valid alternative for its effectiveness and rapidity. The present work stands as a detailed case study of inverse analysis application using the commercial code Hydrus 2D by PC-Progress (Simunek et al. 2006), which is a powerful numerical tool for direct and inverse problems solving. The topic is here addressed through a critical analysis of the indirect simulations output using a quantitative (by means of a set of statistical metrics/indices) and a qualitative approach (plots to compare graphically observed and simulated data).

### 2 The case study

The river Secchia is one of the main right hand tributaries of the river Po, with a length of 172 km and a catchment surface of 2292 km<sup>2</sup>. The riverbank section selected for the present study is located close to the town of Cavezzo (Modena). A topographic survey has been used to trace the section geometry (see Figure 1A). The stratigraphy of the section has been investigated with a series of CPTu tests performed in the berm and in the crest, which were interpreted using the well-known Robertson (2009) SBT (Soil Behaviour Type) charts. Unit A (embankment layer) is an inhomogeneous alternation of silts and sandy silts. Unit A’ (fluvial deposit) consists of coarser sediments deposited during past floods while unit B (foundation) is made of finer material compared to the above layers. Unit C (aquifer) is a slightly coarser layer and it corresponds to the shallow aquifer affected by the changing hydrometric level of the river and the rainfall contribution and it shows greater permeability compared to other layers. Unit D (subsoil), below unit C, is an almost uniform clayey layer.

### 3 The instrumented section

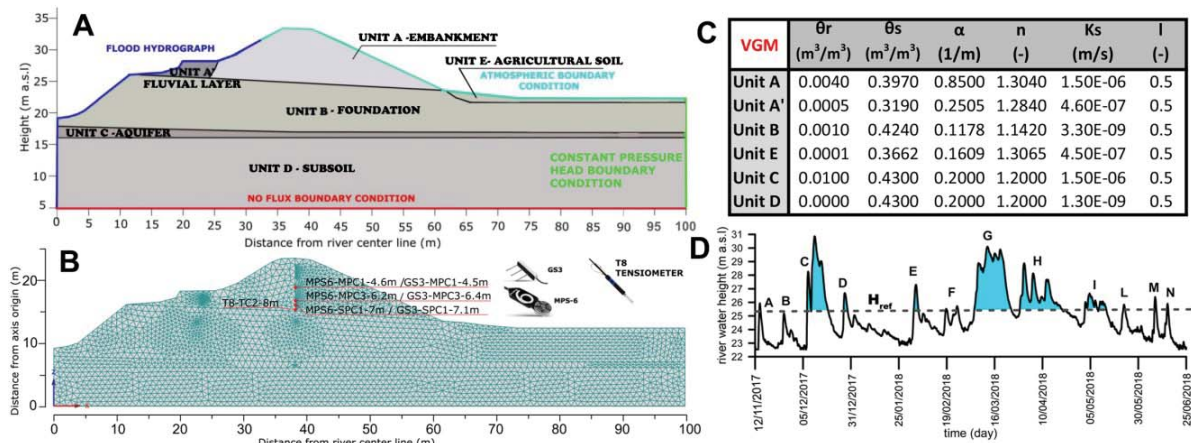


**Figure 1.** (A) Sketched geometry of the investigated section with indication of the soil stratigraphy. (B) Mesh of the FE model of the riverbank section in Hydrus 2D, with indication of the sensors installed in Unit A. (C) Initial set of hydraulic and retention VGM parameters for the FE analysis. (D) riverSecchiahydrograph in correspondence of the investigated section with indication of the reference height ( $H_{ref}$ ). Each flood event is labelled with a letter from A to N.

The embankment was instrumented with 20 sensors (Rocchi et al., 2020) for the measurements of pressure head (from here on “P.h.”), as MPS-6 (Decagon Device) and T8 (UMS), and volumetric water content (“w.c.”), as GS3 (Decagon Device). The sensors were installed in dedicated boreholes, with single or a multiple-point installation. The present study focuses on Unit A parameters optimization; thus, the only eight sensors installed in depth in this layer are considered in the inverse analysis (see Figure 1B). More information on the whole monitoring system, sensors calibration, installation and time series, can be found in Gragnano et al. (2021a).

### 4 The numerical model

The 2D geometry of the investigated riverbank section has been defined in Hydrus 2D code by means of 47 geometrical points. The resulting domain is 100 m wide from the centre of the river bed to the far-field and 23.4 m high from the bottom level to the embankment crest. The origin of the geometrical reference system is the centre of the river bed (x-axis) and 10 m a.s.l (z-axis). Observation points are located in Unit A where sensors have been installed (Figure 1B). The boundary conditions applied to the model are summarised in Figure 1A. To define the atmospheric boundary condition, data of precipitation, evaporation and transpiration every 30 min have been used. Data of humidity, temperature and precipitation are recorded by a weather station in Cortile da Carpi (Lat. 44.778387, Lon. 10.971285), about 7 km away from the investigated section. To compute evaporation and transpiration contribution, the Penman-Monteith method, as revisioned by Allen et al. (1994) has been used. The hydrometric data used for the Dirichlet boundary condition on the left side of the model are collected from the stream gauge at Ponte Motta (Lat. 44.821291, Lon. 10.994664), about 10 km upstream. To the right edge of the model a constant head of  $h=11$  m is assigned to represent the hydrostatic conditions of the far-field water table. The chosen mesh is unstructured and it is composed of 3025 nodes and 5819 2D triangular elements (see Figure 1B). The transient flow through the soil layers in the period from 12<sup>th</sup> November 2017 to 23<sup>rd</sup> June 2018 has been simulated using Hydrus2D. Information on pressure head and volumetric water content from the installed instrumentations at day 0 of the simulation have been used to set the initial conditions. A linear interpolation of these values above (unsaturated zone) and below (saturated zone) the water table has been hypothesized. A tolerance of 0.01 (%%) for w.c. estimation and of 0.05 m for P.h. have been chosen taking into account the precision of the measuring devices installed. 13 evaporation tests have been performed on undisturbed and reconstituted samples at the in situ void ratio in order to investigate the retention and hydraulic parameters of the layers of interests. More information on the laboratory tests performed can be found in Gragnano et al. (2021b). Regarding the analytical models for the retention curve parametrisation, the van Genuchten model (further in the text indicated with the acronym VGM) has been used for the SWRC together with the statistical pore size distribution of Mualem to describe the hydraulic conductivity function  $K(h)$ . In Figure 1C the average values of the retention parameters of the VGM used as set of initial parameters for the direct and indirect simulations (inverse analysis) are presented.

## 5 Analysis of retention parameters

A sensitivity analysis has been performed on the VGM parameters to define the most relevant to be optimized by inverse analysis. To analyse sensitivity, the One Factor A Time Technique (acronym OFAT) has been used: in a system with  $k$  parameters, the value of one parameter is changed (in this case a +/-1% change is applied) and the remaining  $k-1$  parameters must be set to their base value. This technique is widely used due to the reduced computational effort but it does not consider the simultaneous variation (and correlation) of the parameters. To assess the sensitivity of the different retention parameters, the dimensionless sensitivity coefficient calculated according to Simunek et al (1998) has been applied. Considering, for instance, sensor MPS6-SPC1-7m, the retention parameters of Unit A that showed greatest sensitivity in correspondence of the major flood event (22/03/2018) are the saturated water content  $\theta_s$  (with a maximum sensitivity in negative sign of 0.19); the inverse of the air entry value  $\alpha$  (-0.12); the saturated hydraulic conductivity  $K_s$  (-0.25) and the shape parameter  $n$  (-0.66) while the residual water content  $\theta_r$  and the connectivity factor  $l$  have a low sensitivity equal to -0.02 and -0.04, respectively.

## 6 The calibration procedure

The VGM parameters ( $\theta_s, \alpha, K_s, n$ ) of Unit A, that showed a high sensitivity in Section 5, have been calibrated using a local optimization method based on the Levenberg - Marquardt algorithm implemented in the Hydrus package (Simunek et al. 2006). The indirect estimations of the model parameters are obtained from the minimization of a suitable objective function which expresses the discrepancies between observed and simulated data, starting from an initial set of the parameters (presented in Figure 1C) and a dataset of  $n. 7$  observation points from in situ monitoring ( $n. 3$  w.c. sensors and  $n. 4$  P.h. sensors, presented in Figure 1B). The formulation of the objective function implemented in Hydrus2D requires that a weight is assigned to each individual observed data. Two different weighting distributions (indicated hereafter as “w.d.”) have been considered in the performed inverse analysis: a weight equal to unity for all the observed data and a different weight given to each individual data according to the river hydrometric height reached in that flood and its persistence in time (i.e. according to the area associated to each flood in the hydrograph of Figure 1D). A reference river water height ( $H_{ref}$ ) of 25.3m – equal to the height a.s.l of the deepest sensor used in the inverse analysis (T8-TC2-8m) – has been considered in order to subdivide the simulated period in the different flood events (named from A to N, see Figure 1D).  $H_{ref}$  isolates the flood events most notable for the investigated period (cyan areas in Figure 1D) and more likely able to trigger relevant pore water pressure (and water content) changes in Unit A. All the observed data registered in correspondence of a river water height below the reference value have a zero weight. Flood G has the largest area ( $Area_{flood\ G}$ ) and the greatest weight ( $=1$ ), while the others ( $Area_{flood\ k}$ ) have smaller weights ( $w_k$ ) in accordance with the following formulation (equation 1):

$$w_k = \frac{Area_{flood\ k}}{Area_{flood\ G}} \text{ with } k: A \dots N \quad (1)$$

Then, another weight (to be combined with the previous one) has been associated to each observed data according to the variation of records from the maximum value of the considered time-series (P.h. or w.c.) registered during a certain flood event  $k$ , with respect to the whole interval of change (max value-min value). This weight ( $w_{kl}$ ), internal to each flood event and observation point, is calculated as follows (equation 2):

$$w_{kl} = \left| \frac{q_{kl}^* - q_{kl\_max}^*}{q_{kl\_max}^* - q_{kl\_min}^*} \right| \quad (2)$$

where  $q_{kl}^*$  is the observed data belonging to observation point  $l$  in the flood event  $k$ ,  $q_{kl\_max}^*$  and  $q_{kl\_min}^*$  are the maximum and minimum values, respectively, of the P.h. or w.c. data registered during a flood event  $k$  for a certain observation point  $l$ . The more the change in the value of observed data within the flood event is great, the more its weight is increased in relation to the other records for the same flood. Each observation point has a different number of observed data registered for each flood event; in order to give them the same relevance in the inverse analysis, the sum of the weights of the data belonging to each flood has been set the same for each observation point (i.e. considered sensor). To do so an Equalisation Factor (EF) has been introduced. It is defined for each observation point  $l$  belonging to a certain flood event  $k$  as the ratio between the average of the number of observed data (i.e. acquisitions) of all the observation points (considered together) during flood event  $k$  with respect to the sum of the internal weights of observed data belonging to observation point  $l$  during flood event  $k$  (see equation 3).

$$EF_k = \frac{\frac{n_{kl}}{\sum_{l=1}^p n_{kl}}}{\sum_{m=1}^{n_{kl}} w_{klm}} \quad (3)$$

where  $\mathbf{p}$  is the number of considered observation points during flood event  $\mathbf{k}$ ,  $\mathbf{n}_{\mathbf{k}l}$  is the number of acquisitions of observation point  $\mathbf{l}$  during flood event  $\mathbf{k}$  and  $\mathbf{w}_{\mathbf{k}l}$  is the internal weight associated to each acquisition of observation point  $\mathbf{l}$  during flood event  $\mathbf{k}$ . The final weight of each observed data is computed as follows (equation 4):

$$W_{\text{final}} = E F_{\mathbf{k}} * W_{\mathbf{k}l} * W_{\mathbf{k}} \tag{4}$$

Figure 2 presents a schematic representation of the calibration programme performed on the VGM parameters of Unit A, for a total of 56 indirect simulations. In each of the four groups of inverse analysis observation points of typology P.h. or w.c. have been chosen, together with one of the two presented w.d.. From one up to four parameters have been optimized together, for a total of n.14 indirect simulations in each group of inverse analysis.

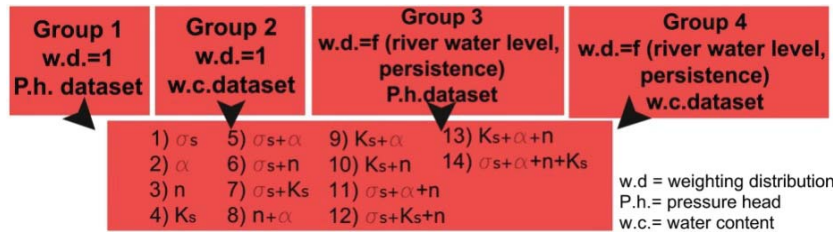


Figure 2. Schematic representation of the calibration programme performed by inverse analysis.

### 7 Results of Inverse Analysis application

Table 1. Set of metrics/indices used for the quantitative performance evaluation of the indirect simulations

Metric/index	Mathematical formulation	Best value /values range	
<b>Modified Index of Agreement (IA<sub>j</sub>)</b>	$IA_j = 1 - \frac{\sum_{j=1}^n  M_i - S_i ^j}{\sum_{j=1}^n ( S_i - \bar{M}  +  M_i - \bar{M} )^j}$	1 [-infinite 1]	$M_i$ observed value $S_i$ simulated value
<b>Modified NSE (NSE<sub>j</sub>)</b>	$NSE_j = 1 - \frac{\sum_{j=1}^n  M_i - S_i ^j}{\sum_{j=1}^n  M_i - \bar{M} ^j} \quad j = 1$	1 [-infinite 1]	$n$ n° of observed data $\bar{M}$ mean observed values $\bar{S}$ mean simulated values
<b>Coefficient of determination (R<sup>2</sup>)</b>	$R^2 = \left\{ \frac{\sum_{i=1}^n (M_i - \bar{M})(S_i - \bar{S})}{\sqrt{\sum_{i=1}^n (M_i - \bar{M})^2} \cdot \sqrt{\sum_{i=1}^n (S_i - \bar{S})^2}} \right\}^2$	1 [0 1]	$\sigma_s = \sqrt{\frac{1}{n} \cdot \sum_{i=1}^n (S_i - \bar{S})^2}$
<b>Root Mean Square Error (RMSE)</b>	$RMSE = \sqrt{\frac{1}{n} \cdot \sum_{i=1}^n (M_i - S_i)^2}$	0 [0 infinite]	
<b>Kling-Gupta efficiency (KGE)</b>	$KGE = 1 - \sqrt{(R - 1)^2 + \left(\frac{\sigma_s}{\sigma_M} - 1\right)^2 + \left(\frac{\bar{S}}{\bar{M}} - 1\right)^2}$	1 [-infinite 1]	$\sigma_M = \sqrt{\frac{1}{n} \cdot \sum_{i=1}^n (M_i - \bar{M})^2}$

16 over 28 indirect simulations using a P.h. dataset have reached convergence (9/17 using a w.d. equal to unity) while 8/28 using a w.c. dataset (4/8 using a w.d. equal to unity). The typical approach adopted to evaluate model performance uses the comparison between simulated output and a dataset of observations. Model performance can be addressed by means of qualitative and quantitative criteria. Quantitative criteria rely on metrics (or indices) and each of them has its pros and cons and the modeller has to choose the best set according to the different sources of uncertainty associated with input data, model structure and parameterization (Bertolini, 2021). The best set is composed of metrics that show direct physical meaning and interpretation, whose trend is consistent with logical directions and (when possible) independent of the measure unit and bounded. A pool of Accuracy Metrics and Efficiency Metrics has been used to analyse the performance of the successful indirect simulations (i.e. simulations that reached convergence in the inverse analysis) in order to individuate the best set/s of optimized parameters. In Table 1 the metrics/indices in use with their mathematical formulation, interval of variation and best fit are presented. As could be observed the modified forms of the Nash-Sutcliffe Efficiency (NSE<sub>j</sub> with j=1) and Index of Agreement (IA<sub>j</sub> with j=1) are preferred over the original formulations, NSE and IA, in order to overcome their oversensitivity to extreme values. Kling-Gupta Efficiency (KGE) represents an improvement of the NSE index because it facilitates the analysis of the relative importance of its different components (correlation, bias and variability), avoiding cross-correlation between bias and variability. Despite the large use made of the coefficient of determination R<sup>2</sup>, it can show illogical behaviour due to the extreme sensitivity to outliers for this reason its use has always to be cautious and coupled with other metrics. For each indirect simulation, the whole pool of presented metrics has been used on the observed-simulated datasets collected over the whole simulation period (November 2017 - June 2018) and over a more restricted period

composed of the major flood events registered (C,G and H in Figure 1D). Metrics values obtained for each indirect simulation have been compared to the ones obtained for base simulation (i.e. the simulation that uses the initial set of parameters). The total enhancement (*T.E.*) in model performance has been computed for each indirect simulation (*j*) as follows (equation 5):

$$T.E. = 0.5 * \sum_i \frac{(p_{ij} - p_{ij_o})}{p_{ij_o}} + 1 * \sum_i \frac{(q_{ij} - q_{ij_o})}{q_{ij_o}} \quad (5)$$

where  $p_{ij}$  is the value of the metric *i* computed for the indirect simulation *j* over the whole simulation period,  $p_{ij_o}$  is the value of the metric *i* computed for the base simulation  $j_o$ ,  $q_{ij}$  is the value of the metric *i* computed for the indirect simulation *j* over the restricted simulation period (C+G+H flood events),  $q_{ij_o}$  is the value of the metric *i* computed for the base simulation  $j_o$  in the same simulation period. The points allocated for the performance of an indirect simulation over the whole simulation period have been considered half the ones computed over the major flooding events (as could be observed in equation 5). This is driven by the aim of the model simulation and the calibration programme performed to give an accurate punctual definition of pore water pressure and water content distribution during major flooding events, when a consistent reduction of the Factor of Safety could be observed, to be used in future stability analyses. The quantitative evaluation of indirect simulations performance has led to the individuation of the two best sets of optimized parameters: the first (Set 1) obtained from an observation dataset of typology P.h. and a w.d. function of persistence and river water height, the second (Set 2) of typology w.c. and w.d. equal to unity.

**Table 2.** The table reports the set of optimized parameters (Set 1 and Set 2) and the initial set of parameters (Set 0)

Unit A	$\theta_r$ (m <sup>3</sup> /m <sup>3</sup> )	$\theta_s$ (m <sup>3</sup> /m <sup>3</sup> )	$\alpha$ (1/m)	$n$ (-)	$K_s$ (m/s)	$l$ (-)
Set 0	0.004	0.3970	0.850	1.304	1.500E-06	0.5
Set 1	0.004	0.5542	1.140	1.269	1.659E-06	0.5
Set 2	0.004	0.3729	0.850	1.304	1.500E-06	0.5

In table 2 the sets of optimized VGM parameters are presented. Set 1 has optimized 4/4 VGM parameters  $\theta_s$ ,  $\alpha$ ,  $n$ ,  $K_s$  with a percentage variation (with respect to the initial value) of 39.6%, 29.9%, -2.9%, 10.6%, respectively. It has been registered an enhancement in the performance in all the four considered P.h. observation points in Unit A, while a poorer performance in 2/3 observation points of typology w.c. (GS3-MPC3-6.4m and GS3-SPC2-7.1m) located in the embankment layer. Set 2 has optimized 1/4 VGM parameters ( $\theta_s$ ) with a low percentage variation of -6% with respect to the initial parameter value. It has been registered a low enhancement in all the three w.c. observation points while any significant change in the four P.h. points. Figure 4 presents a graphical comparison of the performance of the base simulation, Set 1, Set 2 and observed data in 7 different observation points of Unit A. Looking at the inverse analysis results, we can state that the optimization using a P.h. dataset and a w.d. which privileges observed data during high water events produced the best results in the simulation of pwp distribution. It seems extremely difficult to individuate a set of optimized parameters able to enhance the performance of the model both in pwp and w.c. punctual prediction. A choice, based on the final aim of the simulation, has to be made by the modeller prior to the performance of the calibration programme by inverse analysis. These results seem to suggest that the adoption of a mixed dataset of observation points (i.e. observed data of typology P.h. and w.c.) considered together in the inverse analysis, can lead with great probability to low enhancements in both the simulations of P.h. and w.c. distribution in the bank section, as this condition is located mid-way the two analysed ones. This hypothesis has yet to be proved and it is not addressed directly in the present contribution. Figure 3 suggests that the unique flood events that have triggered a significant change in the response of the sensors located in Unit A are floods C,G and H. The availability of observed data from a temporal period with a greater number of significant hydraulic stimuli (flood events) for the sensors located in Unit A, with great probability could have led to more effectiveness in the retention parameters optimization.

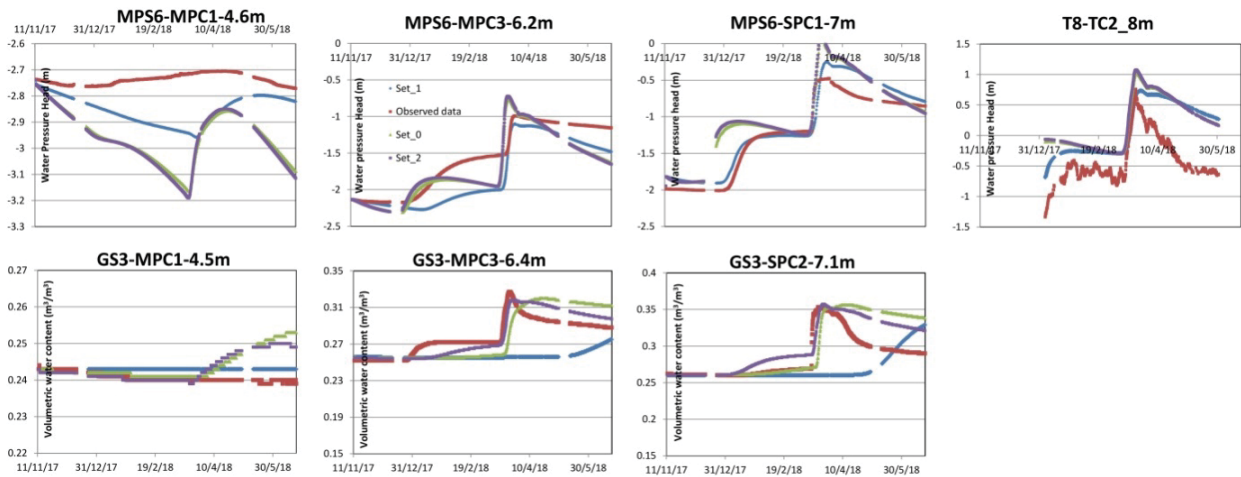


**Figure 3.** Graphical comparison between observed data (red dots), simulated data using the initial set of parameters Set 0 (green dots), using Set 1 (blue dots) or Set 2 (purple dots) of optimized parameters

## 8 Conclusions

The focus of the present work is the analysis of limitations and potentials of applying the inverse analysis to the optimization of model parameters. The problem turned out rather complex, as the chosen section is multi-layered, the period of simulation embraces almost a year of data acquisition and the seepage phenomenon simulated is time dependent. To simplify the parameter optimization, the calibration has been applied to one single layer, Unit A, primarily interested by possible slope instabilities, and only to retention and hydraulic parameters that showed the highest sensitivity. If problem complexity can be reduced, as in the present case study, the Levenberg-Marquardt algorithm has proved to be a valid alternative to classical “trial and error procedures”, showing to be able to increase consistently the reliability of the numerical models. Quantitative methodologies that make use of combinations of various metrics and indices are the required tools when the performance of a large number of indirect simulations is under investigation or when the modeller needs to focus on the behaviour of particular observation points, simulation periods (flood peak, drawdown etc) or soil layers. Therefore, qualitative methodologies could be used only as a complement for the comparison of different model performance.

## Acknowledgments

The authors would like to acknowledge the financial support from MIUR (REDREEF- PRIN 2017 Call, grant 2017YPMBWJ).

## References

- Allen, R.G., Smith, M., Pereira, L.S., Perrier, A. (1994). An update for the calculation of reference evapotranspiration. *ICID Bulletin*.
- Bertolini, I. (2021). A methodological approach for the performance optimization of transient seepage models through inverse analysis. *Ph.D. thesis*.
- Gottardi, G., Gragnano, C.G., Rocchi, I., Bittelli, M. (2016). Assessing River Embankment stability under transient seepage conditions. *VI Italian conference of researchers in Geotechnical Engineering, CNRIG 2016*.
- Gragnano, C.G., Bertolini, I., Rocchi, I., Gottardi, G. (2019) On the stability of a fully instrumented river embankment under transient conditions. *Proceedings of CNRIG 2019. Springer*.
- Gragnano, C.G., Rocchi, I., Gottardi, G. (2021a) Field monitoring and Laboratory testing for an integrated modelling of river embankment under transient conditions. *Geotechnical Geoenvironmental Engineering*, 147(9)
- Gragnano, C.G., Moscarriello, M.G., Sabatino, C., Rocchi, I., Gottardi, G. (2021b). An integrated approach of laboratory testing and field monitoring for the stability analysis of a partially saturated river embankment. *Rivista Italiana di Geotecnica*, 2, 35-54.
- Robertson, P.K. (2009). Interpretation of cone penetration tests - a unified approach. *Can. Geot. J.*, 46(11), 1337-1355.
- Rocchi, I., Gragnano, C.G., Govoni, L., Bittelli, M., Gottardi, G. (2020). Assessing the performance of a versatile and affordable geotechnical monitoring system for river embankments. *Physics and Chemistry of the Earth parts A/B/C*, 117.
- Simunek, J., Sejna, M., van Genuchten, M.T. (2006). The HYDRUS Software Package for Simulating Two- and Three-Dimensional Movement of Water, Heat, and Multiple Solutes in Variably-Saturated Media. *User Manual*.
- Simunek, J., van Genuchten, M.T., Wendroth, O. (1998). Parameter estimation analysis of the evaporation method for determining soil hydraulic properties. *Soil science society of America Journal*, 62(4), 894-905.